

## Reflection of OH molecules from magnetic mirrors

This content has been downloaded from IOPscience. Please scroll down to see the full text.

2008 New J. Phys. 10 053018

(<http://iopscience.iop.org/1367-2630/10/5/053018>)

View [the table of contents for this issue](#), or go to the [journal homepage](#) for more

### Download details:

IP Address: 128.214.163.21

This content was downloaded on 29/08/2016 at 12:18

Please note that [terms and conditions apply](#).

You may also be interested in:

### [Production and deceleration of a pulsed beam](#)

Sebastiaan Y T van de Meerakker, Irena Labazan, Steven Hoekstra et al.

### [A compact design for a magnetic synchrotron to store beams of hydrogen atoms](#)

Aernout P P van der Poel, Katrin Dulitz, Timothy P Softley et al.

### [A Stark decelerator on a chip](#)

Samuel A Meek, Horst Conrad and Gerard Meijer

### [Dependences of slowing results on both decelerator parameters and the new operating mode: taking ND3 molecules as an example](#)

Shunyong Hou, Shengqiang Li, Lianzhong Deng et al.

### [Zeeman deceleration of metastable nitrogen atoms](#)

Katrin Dulitz, Jutta Toscano, Atreju Tauschinsky et al.

### [The formation and interactions of cold and ultracold molecules: new challenges for interdisciplinary physics](#)

O Dulieu and C Gabbanini

## Reflection of OH molecules from magnetic mirrors

Markus Metsälä, Joop J Gilijamse, Steven Hoekstra,  
Sebastian Y T van de Meerakker and Gerard Meijer<sup>1</sup>

Fritz-Haber-Institut der Max-Planck-Gesellschaft, Faradayweg 4-6,  
14195 Berlin, Germany

E-mail: [meijer@fhi-berlin.mpg.de](mailto:meijer@fhi-berlin.mpg.de)

*New Journal of Physics* **10** (2008) 053018 (10pp)

Received 20 February 2008

Published 14 May 2008

Online at <http://www.njp.org/>

doi:10.1088/1367-2630/10/5/053018

**Abstract.** We have reflected a Stark-decelerated beam of OH molecules under normal incidence from mirrors consisting of permanent magnets. Two different types of magnetic mirrors have been demonstrated. A long-range flat mirror made from a large disc magnet has been used to spatially focus the reflected beam in the longitudinal direction ('bunching'). A short-range curved mirror composed of an array of small cube magnets allows for transverse focusing of the reflected beam.

### Contents

<b>1. Introduction</b>	<b>2</b>
<b>2. Experimental set-up</b>	<b>2</b>
<b>3. Results and discussion</b>	<b>6</b>
<b>4. Conclusions</b>	<b>9</b>
<b>Acknowledgments</b>	<b>9</b>
<b>References</b>	<b>9</b>

<sup>1</sup> Author to whom any correspondence should be addressed.

## 1. Introduction

The use of inhomogeneous magnetic fields to influence the trajectories of atoms and molecules in a free flight has played an important role in the development of the field of atomic and molecular beams and has contributed enormously to its success [1]. The manipulation of beams of atoms and molecules with external magnetic fields as it has been used in the past almost exclusively involved the transverse motion of the particles [2, 3]. The reason for this is obvious: the magnetic field gradients that can be realized in the laboratory are sufficient to influence the transverse velocity components of the molecules in the beam, as these are centered around zero velocity. However, the forward velocity of molecules in conventional beams is centered around a large value. Therefore, to be able to influence the longitudinal motion of the molecules slow beams are required.

During recent years a variety of methods have been demonstrated to produce beams of slow molecules. Several of these methods use seeded, pulsed molecular beams as a starting point. In such beams only a limited number of ro-vibrational levels is populated, with a high phase-space density. To reduce the speed of the molecules in the beam, the interaction of the molecules with time-varying electromagnetic fields can be exploited. Thus far, this has been demonstrated for molecules using electric ([4, 5] and references therein) and optical fields [6], and for atoms using magnetic fields [7, 8]. Mechanical means to produce beams of slow molecules have also been demonstrated, e.g. the back-spinning nozzle [9]. Closely related to this are methods that utilize reactive [10] or rotationally inelastic [11] collisions in counter-propagating or crossed beams to produce slow molecules. Alternatively, rather than starting from a pulsed supersonic beam, the low-velocity tail of the thermal Maxwellian velocity distribution in an effusive molecular beam can be filtered out [12]. Via all of these approaches, beams of molecules with kinetic energies on the order of  $1 \text{ cm}^{-1}$  or less can be produced. This is sufficiently low to allow for normal incidence reflection from magnetic mirrors.

In the field of cold atoms, permanent magnets have found many uses, and samples of cold atoms have been reflected, guided and trapped by their potentials [13]. As samples of cold atoms are routinely produced with temperatures in the microkelvin range, the requirements on the magnetic field-strengths are rather relaxed. Periodically magnetized recording media, e.g. video or audio tape, have been used to construct curved mirrors for atoms. In the experiments presented here, we have used beams of ground-state OH molecules, slowed down using a Stark decelerator. These decelerated beams still have a kinetic energy corresponding to a temperature of a few hundred millikelvin, and significantly higher field-strengths are therefore required. We have used rare-earth magnets that can possess a remanence of higher than 1 T. The small size and the low cost of these magnets make them ideally suited to create different types of magnetic mirrors for molecules.

## 2. Experimental set-up

In figure 1 a scheme of the essential part of the experimental set-up is shown. A detailed description of the molecular beam machine, and particularly of the deceleration of a beam of OH molecules, is given elsewhere [14, 15]. In the experiments reported here, a pulsed beam of OH molecules is decelerated from  $390 \text{ m s}^{-1}$  to a velocity in the  $10\text{--}20 \text{ m s}^{-1}$  range using a 119 cm long Stark decelerator consisting of 108 electric field stages; in figure 1 only the last six stages of the Stark decelerator are shown. About 10 mm behind the decelerator, the OH

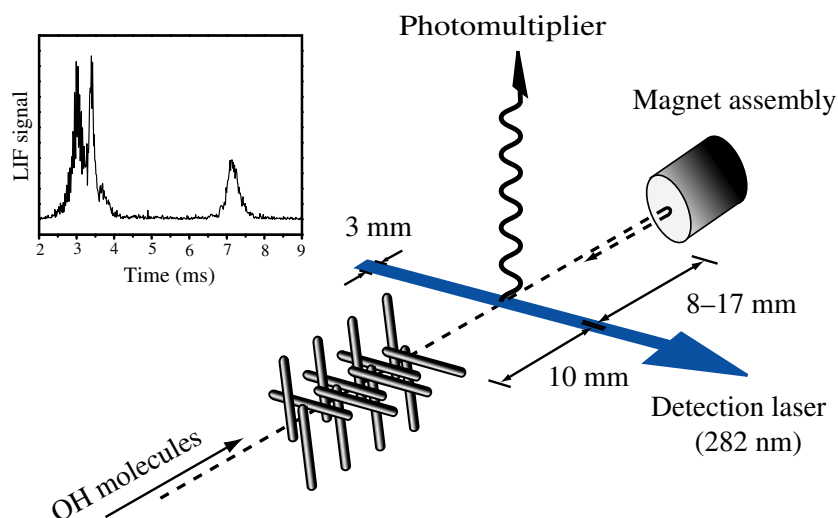


**Figure 1.** A schematic view of the detection zone in the experiment. For clarity, only the last seven electrode pairs of the decelerator are shown. The dashed line indicates the path of the molecular beam. The graph in the upper left corner shows a TOF profile for a beam of ground-state OH molecules decelerated from 390 to 15 m s<sup>-1</sup>. The undecelerated molecules arrive in the detection zone about 3 ms after their production in the source region, whereas the decelerated ones take some 4 ms longer.

molecules pass through the detection zone. Here, the laser-induced fluorescence (LIF) excitation is performed by 282 nm laser light from a pulsed dye laser (5 ns pulse duration and bandwidth of about 0.1 cm<sup>-1</sup>). The  $Q_1(1)$  transition of the  $A^2\Sigma^+, v = 1 \leftarrow X^2\Pi_{3/2}, v = 0$  band is induced and the resulting off-resonant fluorescence to the  $X^2\Pi, v = 1$  state is recorded by a photomultiplier tube. About 2 mJ of laser pulse energy in a 3 mm diameter beam is used, which is sufficient to saturate the transition. The experiment runs at a 10 Hz repetition frequency, and a typical measurement is averaged over 10–1000 shots for improved statistics.

A typical time-of-flight (TOF) measurement for a beam of OH molecules passing through the Stark decelerator beam machine is shown in the upper left corner of figure 1. The undecelerated part of the OH beam arrives in the detection region about 3 ms after its production in the source chamber. Only OH ( $X^2\Pi_{3/2}, v = 0, J = 3/2$ ) molecules in the low-field seeking component with the largest Stark shift, e.g. the  $M_J\Omega = -9/4$  component, are decelerated. In this particular measurement, these molecules are decelerated to a final velocity of 15 m s<sup>-1</sup> and they arrive in the detection region after 7 ms. The decelerated packet contains approximately 10<sup>5</sup>–10<sup>6</sup> OH molecules, has a spatial extent of about 3 mm along the molecular beam axis and is about 4 × 4 mm<sup>2</sup> in the transverse direction at the exit of the decelerator. The full width at half maximum (FWHM) of the velocity spread in the forward direction is about 7 m s<sup>-1</sup>, corresponding to a longitudinal temperature of 10 mK. In the transverse direction, the FWHM velocity spread is slightly less, about 5 m s<sup>-1</sup>. Only this decelerated packet of OH molecules is relevant for the magnetic reflection experiments presented here.

Shortly behind the detection region, two different magnet assemblies can be mounted on a vacuum feedthrough translator that allows to change the distance of the magnet surface to

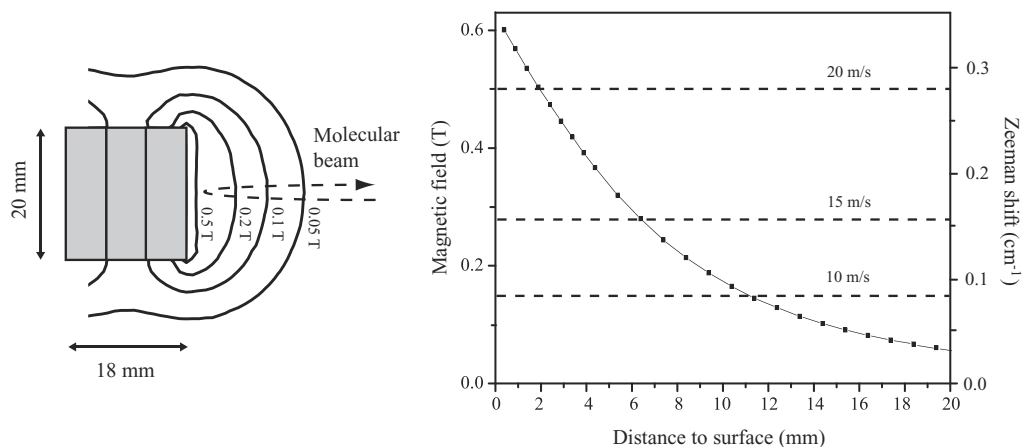


**Figure 2.** Left panel: schematic picture of the disc magnet including calculated iso-magnetic-field lines at 0.05, 0.1, 0.2 and 0.5 T. Right panel: the measured magnetic field strength and the corresponding Zeeman shift for decelerated OH ( $M = +3/2$ ) molecules as a function of distance from the surface of the disc magnet. The dashed horizontal lines indicate the field strengths at which OH molecules with velocities of 10, 15 and 20 m s<sup>-1</sup> will be reflected.

the detection zone from 0 to 30 mm. Ground-state OH molecules are ideally suited for Stark deceleration and subsequent magnetic reflection because they exhibit both a strong Stark shift and a strong Zeeman shift; Stark deceleration followed by magnetoelectrostatic trapping was first demonstrated with OH molecules as well [16]. The interaction potential of the ground-state ( $X^2\Pi_{3/2}$ ,  $J = 3/2$ ) OH molecules with the magnetic field is given by the first-order Zeeman effect. Half of the decelerated OH molecules are in the magnetically high-field seeking states and will be attracted to the magnet, i.e. they will crash into the magnet and be lost for further experiments. The magnetically low-field seeking OH molecules will experience a repulsive force, and after reflection they can pass through the detection region once more. For the  $M = +3/2$  state the Zeeman shift is equal to 0.56 cm<sup>-1</sup> T<sup>-1</sup>. For a magnetic field of 0.5 T this implies that OH molecules with velocities up to a maximum of about 20 m s<sup>-1</sup> can be retro-reflected.

The first magnetic mirror consists of a stack of three disc-shaped nickel coated NdFeB magnets, each with a diameter of 20 mm and a thickness of 6 mm, and is referred to hereafter as the ‘disc magnet’. The remanence of the material used for the magnets is 1.5 T according to the supplier. The measured magnetic field and the corresponding Zeeman shift for the  $M = +3/2$  state along the centerline of the disc magnet as a function of distance from the magnet surface is given in figure 2. The dependence of the magnet field strength on distance from the surface is rather similar for axes that are parallel to and up to a few millimetres away from the centerline; the magnetic field strength only starts to drop off significantly near the edges of the magnet. This mirror therefore acts more or less as a flat mirror. It is observed that the magnetic field has a fairly long range, and that even at distances of a few centimetres from the magnet surface there is still an appreciable magnetic field present. The magnetic field at which OH molecules with velocities of 10, 15 and 20 m s<sup>-1</sup> will be reflected is indicated by the horizontal dashed lines in figure 2. It can be seen that OH molecules with a velocity of 20 m s<sup>-1</sup> will penetrate about 9 mm further into the magnetic field than molecules that move with only half that velocity. This leads to bunching, i.e. a longitudinal spatial focusing, of the reflected molecules.

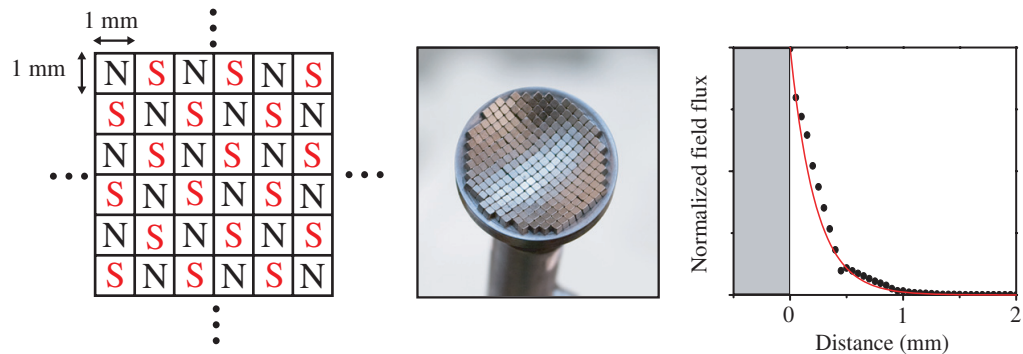


**Figure 3.** Left panel: schematic view of the two-dimensional magnetic array. N and S indicate north and south poles of the individual magnets. Center panel: photograph of the actual array. Right panel: magnetic field strength as a function of distance from the surface of the array. The solid curve is the analytical expression (equation (1)) whereas the dots are the result of a finite element calculation.

The second magnetic mirror is a two-dimensional array of 241 nickel coated  $1 \times 1 \times 1 \text{ mm}^3$  cube NdFeB magnets arranged on a concave round iron substrate with a diameter of 20 mm and a radius of curvature of 20 mm. A photograph of this magnetic mirror, hereafter referred to as the ‘magnet array’, is shown in the center panel of figure 3. The remanence of the material used for the magnets is 1.2 T according to the supplier. The cube magnets are arranged in a checkerboard fashion, with alternating north and south poles in two dimensions, as is schematically depicted in the left panel of figure 3.

If the magnetization varies sinusoidally with a period of  $a$  in the  $(x-y)$ -plane, then the decay of the magnetic field in the  $z$ -direction can be derived similarly as is done for the one-dimensional case [13, 17]. For the two-dimensional case the field strength  $B$  will decay as

$$B = B_0 e^{-\sqrt{2}kz}, \quad (1)$$

where  $B_0$  is the field strength at the surface of the array and  $k = 2\pi/a$ . For our case of  $a = 2 \text{ mm}$ , we have a  $1/e$  decay distance of slightly more than 0.2 mm. We neglect here the higher harmonics of the alternating magnetization and end effects due to the finite number of magnets [18]. To validate this result, we performed a finite element calculation, the result of which is shown in the right panel of figure 3 (dots) together with the predicted field strength from equation (1) (solid curve). As the magnetic field of this mirror extends only over a short range, the molecules will all be reflected at more or less the same distance from the surface, irrespective of their velocities. It is evident, however, that this magnet array forms a transversely focusing mirror with a focal length of 10 mm; after the addition of the magnet array the curvature of the iron substrate is not exactly preserved and the focal distance is actually slightly shorter than this.

An analogous electrostatic mirror, constructed with a one-dimensional array of thin electrodes, has been used to retro-reflect a slow beam of ammonia molecules [19]. A one-dimensional array of small permanent magnets has been used for reflection of cold cesium atoms dropped from an optical molasses [18]. By adding a magnetic bias field to the magnet array, as used here, a two-dimensional array of small traps with large magnetic field gradients can be created [20, 21].

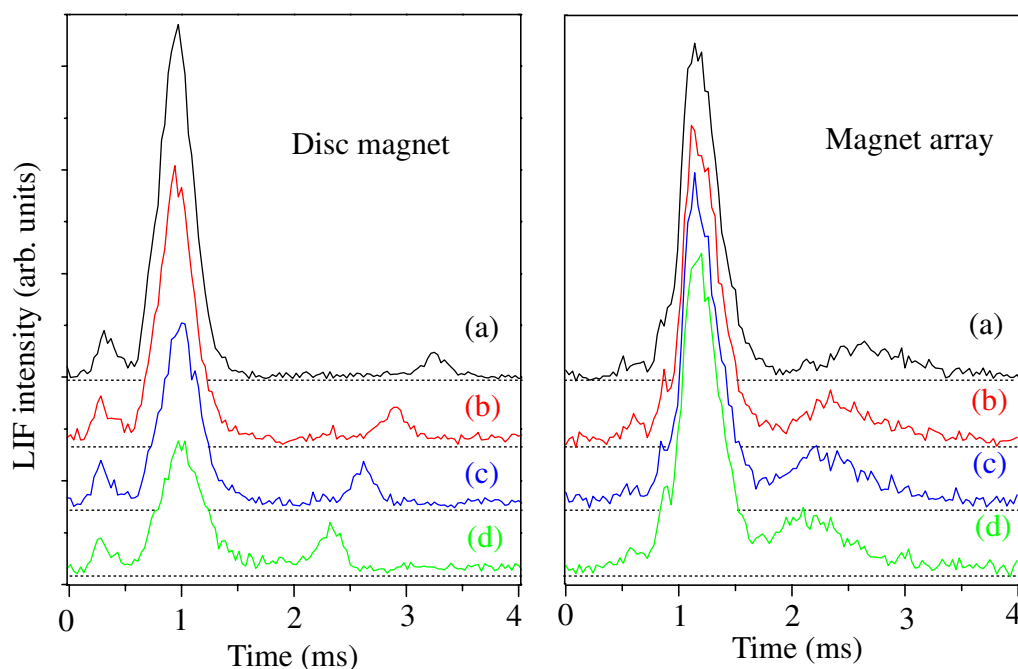


**Figure 4.** Measured TOF profiles for decelerated beams of OH molecules reflected from two different magnetic mirrors. Left panel: OH molecules with a mean velocity of  $19 \text{ m s}^{-1}$  are reflected from the disc magnet. The distance of the surface of the magnet to the detection zone is (a) 17 mm, (b) 13 mm, (c) 10 mm and (d) 8 mm. Right panel: OH molecules with a mean velocity of  $15 \text{ m s}^{-1}$  are reflected from the magnet array. The distance of the surface of the magnet to the detection zone is (a) 13 mm, (b) 11 mm, (c) 10 mm and (d) 8 mm.

### 3. Results and discussion

The left panel of figure 4 shows TOF profiles obtained by reflecting OH molecules from the disc magnet. The data shown are an average over 350 measurements. For convenience, we define the time that the electric fields of the decelerator are switched off, e.g. when the decelerated molecules are near the exit of the decelerator, as  $t = 0$ . The main peak at around 1 ms results from the decelerated packet of OH molecules that passes with a mean velocity of  $19 \text{ m s}^{-1}$  through the detection zone on its way to the magnetic mirror. The reflected packet of molecules returns in the detection zone up to several milliseconds later. The exact arrival time obviously depends on the distance of the magnetic mirror from the detection zone that is varied from 17 via 13 and 10 to 8 mm for curves (a)–(d), respectively. The small peak at around 0.3 ms results from OH molecules that are considerably faster than the decelerated packet, and that will therefore not be reflected. One can see in figure 4 that the height of the main peak at around 1 ms is lower when the magnet surface is placed closer to the detection region. This is due to the less efficient detection of the OH molecules as a consequence of the Zeeman broadening of the detection transition, caused by the long-range field of the disc magnet. In addition, the background signal due to laser light scattered from the disc magnet increases when the magnet is brought closer to the detection zone.

Normally, one would expect the peak of the reflected beam in the TOF profile to be considerably broader than that of the incoming beam, given the longer flight time in combination with the relatively large longitudinal velocity spread in the decelerated beam. The TOF profiles clearly show, however, that the reflected peak is even narrower than the incoming one. This is a direct demonstration of longitudinal spatial focusing of the reflected beam, caused by the long-range field of the disc magnet. The faster molecules penetrate deeper into the magnetic field than the slow ones, and therefore have to travel a longer distance. When the distance of the surface of the disc magnet to the detection region is about 10 mm (c), this results in a catching up of the slow and the fast molecules in the detection region, i.e. in a longitudinal spatial focus in the detection region and in the corresponding narrowest peak in the TOF distribution. Longitudinal spatial focusing, both in real space (bunching) and in velocity space (longitudinal cooling), of a molecular beam using inhomogeneous electric fields has been discussed and demonstrated before [22].

The right panel of figure 4 shows TOF profiles obtained by reflecting OH molecules from the magnet array. The data shown are an average over 660 measurements. Because the strength of the magnetic field is lower than in the case of the disc magnet, the OH molecules are decelerated to a mean velocity of  $15 \text{ m s}^{-1}$  for these experiments. It is seen in figure 4 that the signal due to the incoming slow OH beam remains constant even when the surface of the magnet array is rather close to the detection zone; only the stray light level increases due to light scattering from the magnet array. As expected, there is no evidence of longitudinal spatial focusing of the reflected beam, and the peak of the reflected beam in the TOF distribution is considerably broader than that of the incoming beam. It is interesting to note that for the same distance between the surface of the magnetic mirror and the detection zone, the reflected molecules arrive earlier when reflected from the magnet array than from the disc magnet. This might seem counter-intuitive, as the molecules in this experiment are not only slower to begin with but also approach the surface of the magnet array closer than that of the disc magnet, and therefore have to travel a longer distance. However, with the disc magnet the molecules are gradually decelerated as they approach the magnet and they are accelerated again on their way to the detection region. With the magnet array, on the other hand, the molecules keep a constant speed throughout, with an abrupt change of sign of the velocity vector close to the surface, and therefore actually return earlier to the detection region. We do see an effect of the transverse spatial focusing of the magnet array. For a distance of the surface of the magnet to the detection region of 8 or 10 mm, the ratio of the area of the reflected peak to the initial peak is about a factor two larger for the magnet array than for the disc magnet. This indicates that the molecules are detected more efficiently when reflected from the magnet array due to the transverse focusing of the packet in the detection region.

To further illustrate the effect of longitudinal spatial focusing for the disc magnet, as well as the lack thereof for the magnet array, we have done three-dimensional trajectory calculations to simulate the reflection experiments. Figure 5 shows the measured TOF profiles for both magnetic mirrors, together with the corresponding simulated profiles. In the simulation for the disc magnet the measured magnetic field as given in figure 2 is taken, whereas for the magnet array the analytical expression of equation (1) with  $B_0 = 0.3 \text{ T}$  is used. The shape and time of arrival of the reflected peak is reproduced well in the simulated TOF profiles for both magnetic mirrors. On the right-hand side of figure 5 snap-shots of the longitudinal phase-space distributions of the OH molecules are shown at 0.25 ms time intervals during the reflection process. As the OH molecules approach the surface of the disc magnet, the fast molecules are

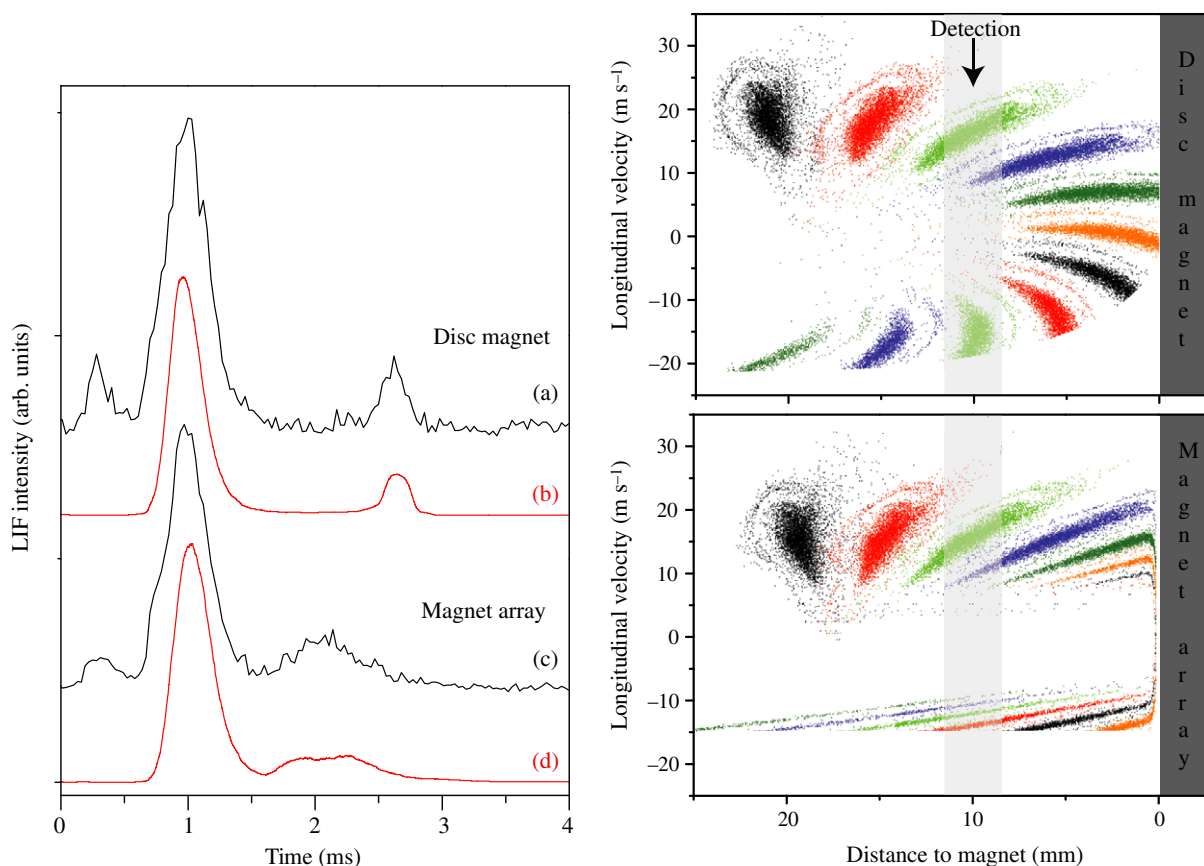


**Figure 5.** Left panel: measured (a,c) and simulated (b,d) TOF profiles for decelerated OH molecules reflected from the two different magnetic mirrors. An OH beam with a mean velocity of  $19 \text{ m s}^{-1}$  ( $15 \text{ m s}^{-1}$ ) is reflected from the disc magnet (magnet array). The distance of the surface of the magnetic mirror to the detection zone is 10 mm. Right panel: snapshots of the corresponding simulated longitudinal phase-space distributions at 0.25 ms time intervals. The position of the detection laser is indicated in gray.

decelerated more than the slow ones and as a result the velocity distribution narrows down while the position distribution broadens. After turning around the opposite happens and the spatial distribution comes to a focus in the detection region. In the reflection process, the initial phase-space distribution of the decelerated packet is more or less reconstructed at the detection zone, but spatially compressed (and therefore slightly extended in velocity space) and rotated by  $180^\circ$ . The clipping of the phase-space distributions at velocities of about  $-21 \text{ m s}^{-1}$  results from the finite height of the magnetic field at the surface; faster molecules have simply not been reflected but have crashed into the surface. The phase-space distributions for the OH molecules that are reflected from the magnet array clearly show that, after an abrupt reversal of the velocity close to the surface, the reflected packet continues to spread out and that no bunching occurs.

#### 4. Conclusions

We have demonstrated reflection of slow beams of OH molecules from two different types of magnetic mirrors, composed of permanent magnets. A long-range flat mirror is used for longitudinal spatial focusing of the reflected molecules whereas a short-range curved mirror is used for transverse focusing.

Permanent magnets with typical magnetic field strengths of 1 T can be custom-made in a wide variety of geometries. They are compact and relatively cheap and can be a viable alternative to electromagnets in the manipulation and control of cold molecules. Apart from magnetic mirrors, magnetic guides and magnetic traps can be made from these permanent magnets as well; the group of Jun Ye (JILA, Boulder, CO, USA) has recently demonstrated magnetic trapping of the OH molecules using an arrangement of permanent magnets [23]. Even though permanent magnets do not allow for rapid tuning of the magnetic field strength, often the strength of the interaction of molecules with the magnetic field can be tuned by (laser) preparation of the molecules in an appropriate quantum state. For molecules in a  $^2\Pi$  electronic state like OH, the magnetic field interaction can even effectively be switched off by transferring the molecules from the  $^2\Pi_{3/2}$  to the  $^2\Pi_{1/2}$  electronic state. When the transfer of molecules is performed via laser excitation followed by spontaneous fluorescence, this scheme allows for the accumulation of Stark-decelerated molecules in an electrostatic trap that is superimposed on the magnetic reflection field, i.e. a more general version of the previously proposed accumulation scheme [24].

#### Acknowledgments

We acknowledge the technical support from Manfred Erdmann. MM is grateful to the Academy of Finland for financial support.

#### References

- [1] Scoles G (ed) 1988 and 1992 *Atomic and Molecular Beam Methods* vol 1 and 2 (New York: Oxford University Press)
- [2] Gerlach W and Stern O 1922 *Z. Phys.* **9** 353
- [3] Rabi I I, Millman S, Kusch P and Zacharias J R 1939 *Phys. Rev.* **55** 526
- [4] Bethlem H L, Berden G and Meijer G 1999 *Phys. Rev. Lett.* **83** 1558
- [5] Heiner C E, Bethlem H L and Meijer G 2006 *Phys. Chem. Chem. Phys.* **8** 2666
- [6] Fulton R, Bishop A I, Shneider M N and Barker P F 2006 *Nat. Phys.* **2** 465
- [7] Vanhaecke N, Meier U, Andrist M, Meier B H and Merkt F 2007 *Phys. Rev. A* **75** 031402
- [8] Narevicius E, Parthey C G, Libson A, Narevicius J, Chavez I, Even U and Raizen M G 2007 *New J. Phys.* **9** 358
- [9] Gupta M and Herschbach D 1999 *J. Phys. Chem. A* **103** 10670
- [10] Liu N-N and Loesch H 2007 *Phys. Rev. Lett.* **98** 103002
- [11] Elioff M S, Valentini J J and Chandler D W 2003 *Science* **302** 1940
- [12] Rangwala S A, Junglen T, Rieger T, Pinkse P W H and Rempe G 2003 *Phys. Rev. A* **67** 043406
- [13] Hinds E A and Hughes I G 1999 *J. Phys. D: Appl. Phys.* **32** R119
- [14] van de Meerakker S Y T, Smeets P H M, Vanhaecke N, Jongma R T and Meijer G 2005 *Phys. Rev. Lett.* **94** 023004
- [15] van de Meerakker S Y T, Vanhaecke N and Meijer G 2006 *Annu. Rev. Phys. Chem.* **57** 159

- [16] Sawyer B C, Lev B L, Hudson E R, Stuhl B K, Lara M, Bohn J L and Ye J 2007 *Phys. Rev. Lett.* **98** 253002
- [17] Opat G I, Wark S J and Cimmino A 1992 *Appl. Phys. B* **54** 396
- [18] Sidorov A I, McLean R J, Rowlands W J, Lau D C, Murphy J E, Walkiewicz M, Opat G I and Hannaford P 1996 *Quantum Semiclass. Opt.* **8** 713
- [19] Schulz S A, Bethlem H L, van Veldhoven J, Küpper J, Conrad H and Meijer G 2004 *Phys. Rev. Lett.* **93** 020406
- [20] Sinclair C D J, Retter J A, Curtis E A, Hall B V, Llorente G I, Eriksson S, Sauer B E and Hinds E A 2005 *Eur. Phys J. D* **35** 105
- [21] Gerritsma R, Whitlock S, Fernholz T, Schlatter H, Luigjes J A, Thiele J-U, Goedkoop J B and Spreeuw R J C 2007 *Phys. Rev. A* **76** 033408
- [22] Crompvoets F M H, Jongma R T, Bethlem H L, van Roij A J A and Meijer G 2002 *Phys. Rev. Lett.* **89** 093004
- [23] Jun Ye 2008 private communication
- [24] van de Meerakker S Y T, Jongma R T, Bethlem H L and Meijer G 2001 *Phys. Rev. A* **64** 041401